

Purification, Functional Reconstitution, and Characterization of the *Saccharomyces cerevisiae* Isoprenylcysteine Carboxymethyltransferase Ste14p* ◆

Received for publication, September 8, 2004, and in revised form, December 14, 2004
Published, JBC Papers in Press, December 20, 2004, DOI 10.1074/jbc.M410292200

Jessica L. Anderson‡, Hilary Frase‡§, Susan Michaelis¶, and Christine A. Hrycyna‡||

From the ‡Department of Chemistry and the Purdue Cancer Center, Purdue University, West Lafayette, Indiana 47907 and the ¶Department of Cell Biology, The Johns Hopkins University School of Medicine, Baltimore, Maryland 21205

Numerous proteins, including Ras, contain a C-terminal CAAX motif that directs a series of three sequential post-translational modifications: isoprenylation of the cysteine residue, endoproteolysis of the three terminal amino acids and α -carboxyl methylesterification of the isoprenylated cysteine. This study focuses on the isoprenylcysteine carboxymethyltransferase (Icmt) enzyme from *Saccharomyces cerevisiae*, Ste14p, the founding member of a homologous family of endoplasmic reticulum membrane proteins present in all eukaryotes. Ste14p, like all Icmts, has multiple membrane spanning domains, presenting a significant challenge to its purification in an active form. Here, we have detergent-solubilized, purified, and reconstituted enzymatically active His-tagged Ste14p from *S. cerevisiae*, thus providing conclusive proof that Ste14p is the sole component necessary for the carboxymethylation of isoprenylated substrates. Among the extensive panel of detergents that was screened, optimal solubilization and retention of Ste14p activity occurred with *n*-dodecyl- β -D-maltoside. The activity of Ste14p could be further optimized upon reconstitution into liposomes. Our expression and purification schemes generate milligram quantities of pure and active Ste14p, which is highly stable under many conditions. Using pure reconstituted Ste14p, we demonstrate quantitatively that Ste14p does not have a preference for the farnesyl or geranylgeranyl moieties in the model substrates *N*-acetyl-*S*-farnesyl-L-cysteine (AFC) and *N*-acetyl-*S*-geranylgeranyl-L-cysteine (AGGC) *in vitro*. In addition to catalyzing methylation of AFC, we also show that purified Ste14p methylates a known *in vivo* substrate, Ras2p. Evidence that metals ions are required for activity of Ste14p is also presented. These results pave the way for further characterization of pure Ste14p, as well as determination of its three-dimensional structure.

zyme responsible for the carboxymethylation step of CAAX protein processing. Icmt recognizes both farnesylated and geranylgeranyl substrates (1–9). Carboxymethylation is critical for the proper localization of Ras proteins in yeast and mouse cells (7, 10, 11) and may also influence the interaction between Ras and other proteins (12). Furthermore, it has recently been determined that prenylated and proteolyzed but unmethylated Ras is not able to promote cellular transformation (13). These findings have led to the hypothesis that Icmt enzymatic activity represents an excellent target for cancer chemotherapeutic intervention. Targeted inhibition of Icmt in cancer cells could be an effective chemotherapeutic strategy for Ras-based cancers.

Ste14p, the Icmt from *Saccharomyces cerevisiae*, identified through genetic and biochemical means, is the founding member of the Icmt family (7, 12, 14, 15). This 26-kDa polytopic integral membrane protein is localized to the membrane of the ER with the bulk of the protein cytosolically disposed (Fig. 1A) (8, 16). This enzyme is comprised of multiple membrane spanning segments and must accommodate chemically diverse methyl donor and acceptor molecules: the hydrophilic *S*-adenosylmethionine (SAM) and a lipophilic isoprenylated protein, respectively. Strikingly, Icmt shares none of the conserved consensus sequences described for known soluble (protein or nucleic acid) methyltransferases (17), suggesting that Icmt may have a distinct type of SAM binding site, as well as a potentially novel catalytic mechanism. The yeast and human Icmts share 41% identity and 63% similarity overall, suggesting that their three-dimensional structures and mechanisms of action are similar. In fact, human Icmt expressed in yeast complements a *ste14* Δ deletion (6), suggesting that yeast Ste14p studies are directly relevant to our understanding of the function and mechanism of human Icmt.

Studies presented here show that high level protein expression in yeast combined with surveying a varied panel of detergents offers an excellent approach to identifying conditions appropriate for the solubilization of functional Ste14p, which may be generally applicable to numerous membrane proteins from yeast or heterologous sources. His-tagged Ste14p expressed from a strong constitutive promoter is overexpressed to levels 20-fold higher than described previously, suggesting that

Isoprenylcysteine carboxymethyltransferase (Icmt)¹ is a polytopic endoplasmic reticulum (ER) membrane-localized en-

* This work was supported by the National Pancreas Foundation (to C. A. H.) and the Purdue Cancer Center. The costs of publication of this article were defrayed in part by the payment of page charges. This article must therefore be hereby marked "advertisement" in accordance with 18 U.S.C. Section 1734 solely to indicate this fact.

◆ This article was selected as a Paper of the Week.

§ Present address: Dept. of Chemistry, Case Western Reserve University, Cleveland, OH 44106.

|| To whom correspondence should be addressed: Dept. of Chemistry, Purdue University, 560 Oval Dr., West Lafayette, IN 47907-2084. Tel.: 765-494-7322; Fax: 765-494-0239; E-mail: hrycyna@purdue.edu.

¹ The abbreviations used are: Icmt, isoprenylcysteine carboxymethyltransferase; AFC, *N*-acetyl-*S*-farnesyl-L-cysteine; AGGC, *N*-acetyl-*S*-

geranylgeranyl-L-cysteine; DDM, *n*-dodecyl- β -D-maltopyranoside; SAM, *S*-adenosyl-L-methionine; ¹⁴C-SAM, *S*-adenosyl-L-[¹⁴C-methyl]methionine; PGK, 3'-phosphoglycerate kinase; AEBSF, aminoethylbenzenesulfonyl fluoride hydrochloride; HRP, horseradish peroxidase; MES, 2-morpholinoethanesulfonic acid; OP, *o*-phenanthroline; Zincon, 2-carboxy-2'-hydroxy-5'-sulfoformazylbenzene; PC, phosphatidylcholine; PE, phosphatidylethanolamine; PS, phosphatidylserine; PA, phosphatidic acid; PI, phosphatidylinositol; CHAPS, 3-[(3-cholamidopropyl)-dimethylammonio]-1-propanesulfonate; α , anti; FTase, farnesyltransferase.

with a 10× histidine tag at the N terminus under the control of the constitutive 3'-phosphoglycerate kinase (PGK) promoter. A 734-bp *EagI*-*SacII* fragment containing the *STE14* gene was amplified from pSM187 and cloned into the *EagI* and *SacII* sites of pCHH10m3N and pCHH10m6N to produce pCHH10m3N-*STE14* and pCHH10m6N-*STE14*, respectively. These plasmids encode Ste14p with a 10× histidine tag followed by a 3 or 6 *myc* epitope repeat at the N terminus. Both are under the control of the constitutive PGK promoter. A 725-bp *XmaI*-*BamHI* fragment containing *STE14* was amplified from pSM187 and cloned into the *XmaI* and *BamHI* sites of pCHH10C to yield pCHH10C-*STE14*. This plasmid encodes Ste14p with a 10× histidine tag at the C terminus, which is under the constitutive control of the PGK promoter. A 724-bp *XmaI* fragment containing *STE14* was amplified from pSM187 and cloned into the *XmaI* site of pCHm3H10C and pCHm6H10C to produce pCHm3H10C-*STE14* and pCHm6H10C-*STE14*, respectively. These plasmids encode Ste14p with either a 3 or 6 *myc* epitope repeat followed by a 10× histidine tag at the C terminus. Both are under the control of the constitutive PGK promoter. A 727-bp *BamHI*-*SacII* fragment containing *STE14* was amplified from pSM187 and cloned into the *BamHI* and *SacII* sites of pSM703 to yield pSM703-*STE14*. This plasmid encodes untagged Ste14p that will be expressed under the PGK promoter. A 975-bp *EagI*-*SacII* fragment containing the *RAS2* gene was amplified from pSM1326 and cloned into the *EagI* and *SacII* sites of pCHH10m3N to produce pCHH10m3N-*RAS2*. This plasmid encodes Ras2p with a 10× histidine tag followed by a 3 *myc* epitope repeat at the N terminus expressed under the control of the PGK promoter. Transformation of this plasmid into the *STE14* deletion strain SM1188 yields strain CH2765, expressing farnesylated, proteolyzed but unmethylated His-Ras2p. All plasmids were sequenced bidirectionally to confirm the DNA sequence.

Isolation of Membrane Fraction from Yeast Cells—Mid-log phase yeast cells ($2.0 A_{600}/\text{ml}$), grown in SC-URA medium, were harvested by centrifugation at $3500 \times g$ for 10 min at 4 °C, washed with 10 mM Na₂S₂O₈, and resuspended in lysis buffer (0.3 M sorbitol, 10 mM Tris-HCl, pH 7.5, 0.1 M NaCl, 5 mM MgCl₂, 1% aprotinin, 10 μg/ml leupeptin, 10 μg/ml pepstatin A, 10 μg/ml chymostatin, 10 μg/ml bestatin, 1 mM dithiothreitol, and 2 mM AEBSF) to a final concentration of 400 A_{600}/ml . After a 15-min incubation on ice, the cells were frozen and thawed twice in liquid N₂. The cells were then lysed by passing the mixture twice through a French press at 18,000 p.s.i. The resultant mixture was centrifuged at $500 \times g$ to remove whole cells and other particulate. Subsequently, the supernatant was treated with 50 units/ml micrococcal nuclease followed by centrifugation at $150,000 \times g$ for 90 min at 4 °C, to pellet the membrane fraction. The pellet was resuspended in lysis buffer containing 10% glycerol, aliquoted, and stored at -80 °C. Membrane protein concentration was determined using Coomassie Plus protein assay reagent (Pierce).

Detergent Solubilization of Crude Membranes—His-Ste14-containing membranes were resuspended in lysis buffer containing 1% detergent to a final protein concentration of 5 mg/ml and incubated with rotation at 4 °C for 1 h. The solution was subsequently centrifuged at $300,000 \times g$ for 30 min at 4 °C, to remove the non-solubilized membrane fraction. The concentration of the protein present in the supernatant was determined by the Amido Black protein assay.

Purification of His-Ste14p from Crude Membranes—His-Ste14p-containing membranes were solubilized as described above in 1% DDM, 20 mM imidazole, pH 8.0, and lysis buffer containing 10% glycerol at a final protein concentration of 5 mg/ml. The $300,000 \times g$ supernatant containing solubilized Ste14p (post-spin) was rocked for 1 h with Talon metal affinity resin beads (Clontech, Inc., Palo Alto, CA), and the beads were then washed twice with Buffer A (lysis buffer plus 10% glycerol, 1% DDM, and 40 mM imidazole), once with Buffer B (Buffer A plus 0.5 M KCl), and once with Buffer C (lysis buffer plus 10% glycerol, 0.1% DDM, 40 mM imidazole, and 0.5 M KCl). The beads were eluted sequentially using lysis buffer containing 10% glycerol, 0.1% DDM, and either 100 mM, 500 mM, or 1 M imidazole. Subsequent to these sequential elutions, the column was stripped with 0.5 M EDTA, pH 8.0. To ensure that all of the His-Ste14p from the postspin fraction was extracted, the flow-through from the first bead column was incubated with fresh beads and the entire process was repeated. All elutions were combined and concentrated in Microcon 30 concentrators (Millipore Co., Billerica, MA). Protein concentration was determined by the Amido Black protein assay (19).

Purification of His-Ras2p from Lysate—Cells expressing CH2765 (His-Ras2p) were resuspended in lysis buffer, frozen, and thawed twice in liquid nitrogen and lysed by passing mixture twice through a French press at 18,000 p.s.i. After spinning at $500 \times g$ to remove cellular debris, glycerol was added to the supernatant to a final concentration of 10%.

This supernatant was then transferred to Talon metal affinity resin beads. The purification procedure continued as described above for His-Ste14p with two modifications. First, the His-Ras2p purification does not contain any detergent. Second, instead of sequential imidazole elutions, His-Ras2p was eluted from the column with EDTA elution buffer (200 mM EDTA, pH 8.0, 10% glycerol, 0.18 M sorbitol, 6 mM Tris-HCl, pH 7.5, 3 mM MgCl₂, 0.6% aprotinin, 6 μg/ml leupeptin, 6 μg/ml pepstatin A, 6 μg/ml chymostatin, 6 μg/ml bestatin, and 1.2 mM AEBSF). It is known that EDTA does not inhibit Ste14p activity. Protein concentration was determined by Coomassie Plus protein assay reagent (Pierce).

Preparation of Liposomes—Lipid mixtures were dissolved in chloroform and dried as a thin film in round bottom flasks under a gentle nitrogen stream. To ensure removal of all chloroform, the lipid films were additionally dried under vacuum for at least 1 h. The lipid films were rehydrated with water or 600 mM Tris-HCl, pH 7.5, to a final concentration of 10 mg/ml. Liposomes were extruded to a diameter of 100 nm with a mini-extruder (Avanti Polar Lipids, Inc.).

Reconstitution of Purified His-Ste14p—The purified protein was reconstituted by rapid dilution (20). A 100–1000-fold weight:weight excess of the liposomal mixtures was added directly to the purified His-Ste14p fraction after elution from the metal affinity column in the presence of AFC and incubated on ice for 5 min. Subsequently, the solution was subjected to a 20-fold rapid dilution in detergent-free buffer.

Immunoblot Analysis—Protein samples containing 1× SDS-PAGE sample buffer were heated to 65 °C for 15 min and resolved by 12% SDS-PAGE. Proteins were transferred to a pure nitrocellulose membrane (0.2 μm; Schleicher & Schuell) at 400 mA for 1 h. The filter was blocked with 20% milk in phosphate-buffered saline with Tween 20 (PBST: 137 mM NaCl, 2.7 mM KCl, 4 mM Na₂HPO₄, 1.8 mM KH₂PO₄, and 0.05% Tween 20, pH 7.4). The filter was then incubated with the primary antibody (1:1000 α-Ste14, 1:2000 α-His or 1:10,000 α-*myc*) dissolved in 5% milk in PBST. Following several washes with PBST, the filter was incubated with the secondary antibody (1:4000 goat α-mouse HRP or 1:10,000 goat α-rabbit HRP) dissolved in 5% milk in PBST. After washing with PBST, the protein bands were visualized by chemiluminescence (SuperSignal West Pico chemiluminescent substrate (Pierce)).

In Vitro Vapor Diffusion Methyltransferase Assay—The assay was performed as described previously (14) except that the reaction generally contained 5 μg of total membrane protein, 200 μM AFC or AGGC as the methyl acceptor, 100 mM Tris-HCl, pH 7.5, and 20 μM SAM (50–60 mCi/mmol). Assays containing purified and reconstituted His-Ste14p typically used less than 1 μg of protein and used 100 mM MES, pH 7.0. Reactions were assembled on ice and incubated for 30 min at 30 °C. Where indicated, samples were processed through a spin column gel filtration step as described below prior to assaying for activity. Inhibition of purified His-Ste14p activity was performed by incubating the reconstituted protein with inhibitor for 10 min at 30 °C prior to addition of SAM.

Determination of His-Ste14p Substrate Specificity—*Escherichia coli* bulk polar lipid plus 0.05% Texas Red 1,2-dihexadecanoyl-*sn*-glycero-3-phosphoethanolamine, triethylammonium salt (Molecular Probes, Eugene, OR) were dissolved in chloroform and dried in a round bottom flask under gentle nitrogen stream. After 1 h under vacuum, the lipid film was hydrated with water to a final lipid concentration of 12.5 mg/ml. These liposomes were extruded to 100 nm diameter. Liposomes were incubated for 5 min with varying amounts of either AFC or AGGC. Water was then added to make the final concentration of lipid 4 mg/ml. This lipid mixture was allowed to equilibrate at room temperature for 15 min. The mixture was then spun through a 600 μl of Sephacryl S-100 high resolution (Amersham Biosciences) column in a 1-ml syringe using glass wool as a frit for 2 min at $1100 \times g$ to remove isoprenylated substrate not incorporated into the liposomes. Actual elution of the vesicles takes place on the order of ~10 s during the spin. Monitoring of the Texas Red concentration at 585 nm verified nearly complete recovery of liposomes at a relatively constant concentration in the column flow-through. These liposomes were immediately subjected to the *in vitro* vapor diffusion methyltransferase assay as described above using 25 μl of the liposome mixture and 0.089 μg of purified His-Ste14p. Each individual concentration of isoprenylated substrate in the liposomes was repeated three times, and each replicate was assayed twice in the methyltransferase assay. The concentration of isoprenylated substrate in the liposomes was determined by ultraviolet absorbance at 207 nm using the zero point as the blank. These values were compared with AFC and AGGC standard curves that contained the same amount of lipid to determine the actual isoprenylated substrate concentration of

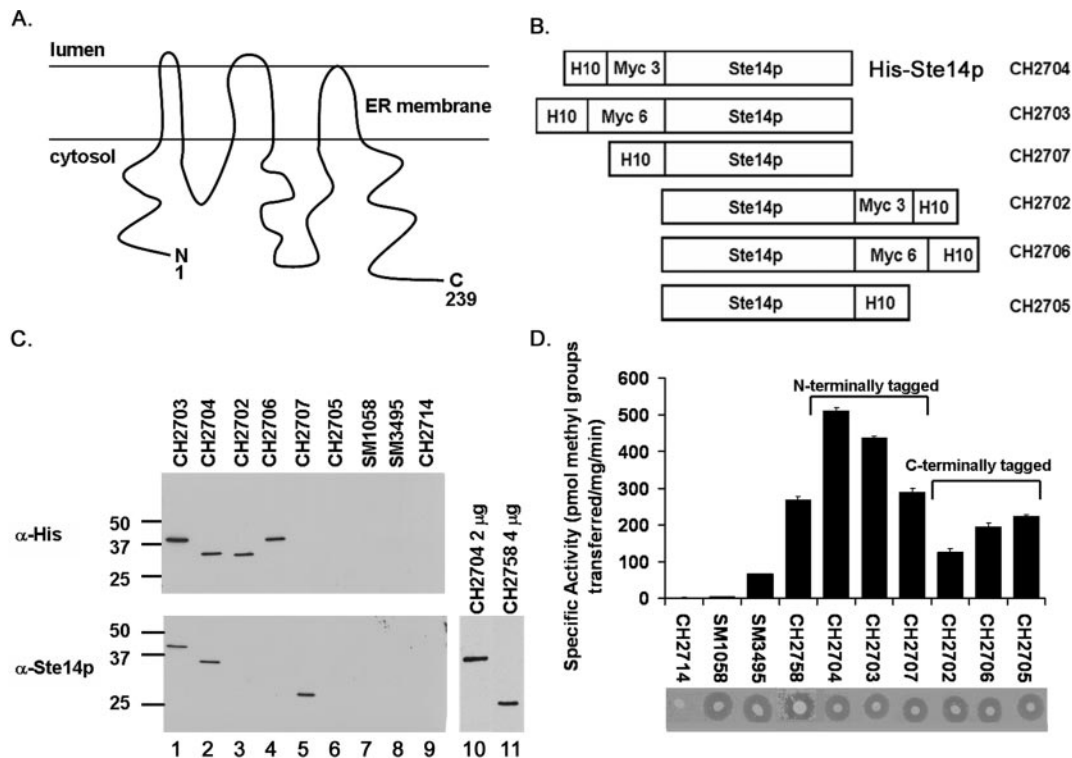


FIG. 1. A, two-dimensional topological model of Ste14p. Schematic representation of the membrane of the endoplasmic reticulum (16). B, epitope-tagged Ste14p constructs. Schematic representation of the six Ste14p constructs used in this study. Each contains a 10× histidine tag (H10) with or without a 3× (Myc 3) or 6× (Myc 6) myc epitope tag repeat at either the N or C terminus. Each tagged construct is expressed behind the constitutive PGK promoter. C, immunodetection of Ste14p. One μg of total protein from each crude membrane preparation was subjected to SDS-PAGE analysis, and Ste14p was visualized by immunodetection with either α-His (1:2000) or α-Ste14 (1:1000) antibodies. Protein bands were visualized by enhanced chemiluminescence following incubation with HRP conjugated secondary antibodies (α-mouse 1:4000 for α-His and α-rabbit 1:10000 for α-Ste14). D, *in vitro* methyltransferase activity of Ste14p in crude membranes. Five μg of total protein from crude membrane preparations were incubated with 20 μM ¹⁴C-SAM (S-adenosyl-L-[¹⁴C-methyl]methionine) and 200 μM AFC for 30 min at 30 °C and activity quantified by the *in vitro* vapor diffusion methyltransferase assay as described under “Experimental Procedures.” CH2714 is a Δ*ste14* strain containing the empty vector, CH2758 is untagged Ste14p behind the 3′-PGK promoter, SM1058 is a wild-type MATa strain expressing wild-type Ste14p endogenously, and SM3495 is a Δ*ste14* strain expressing wild type Ste14p behind the endogenous STE14 promoter. Data are the average of three experiments done in duplicate. Error bars represent ± 1 S.E. Lower panel, *in vivo* activity of Ste14p constructs by halo assay. One μl of a saturated overnight culture of each Ste14p strain and the Δ*ste14* deletion (CH2714) was spotted onto a lawn of MATa cells supersensitive to a-factor (SM2375). A clear zone or halo results from growth arrest of the lawn and is indicative of proper a-factor processing by the strain, which requires functional Ste14p.

each point. Points from several determinations were plotted on one graph and the data were fitted to the Michaelis-Menten equation using GraphPad Prism 4.0. The AFC curves and fit were obtained from 312 data points, representing 26 different concentrations and the AGGC curves and fit were obtained from 288 data points, representing 24 different concentrations.

In Vivo a-Factor Halo Assay—The assay was performed as described previously (16) with the exception that YPD plates containing 0.04% Triton X-100 were used to increase the diffusion of mature a-factor (21). A clear zone, or halo, indicates the secretion of mature a-factor by the MATa cells which in turn inhibits the growth of the lawn, which is supersensitive to mature a-factor.

RESULTS

Versatile Vectors for High Level Expression of Ste14p in S. cerevisiae—To facilitate this project, a basic set of expression tools were established, which allow us to generate large amounts of protein for biochemical and biophysical analyses. We have constructed a series of six *S. cerevisiae* Ste14p expression plasmids that are engineered to contain polyhistidine and multiple myc epitope tags at either the N or C terminus of Ste14p (Fig. 1B). These constructs, as well as the untagged Ste14p protein, are expressed using the strong constitutive PGK promoter. These vectors have been engineered such that any protein of interest can be inserted in frame in the multiple cloning site.

Epitope-tagged Ste14p Proteins Are Expressed at High Levels and Are Biochemically Active in Vitro—We have successfully

utilized these new vectors to generate strains expressing tagged and untagged versions of Ste14p. The polyhistidine tag is used to facilitate purification and the myc tag is used for immunoblot detection. These proteins are expressed, as demonstrated by immunoblotting with an anti-Ste14 polyclonal antibody and commercially available anti-myc and anti-His-tag antibodies (Fig. 1C). Ste14p variants tagged at the N terminus (Fig. 1C, lanes 1, 2, and 5), but not the C terminus (Fig. 1C, lanes 3 and 4), are recognized by a polyclonal anti-Ste14p antibody made against the C-terminal 42 residues of Ste14p (8). The C-terminally tagged Ste14p proteins are not recognized by this antibody presumably because the epitope tags mask or otherwise disrupt recognition of the epitope. Similarly, the polyhistidine epitope appears to be masked in the N-terminally tagged construct CH2707 (Fig. 1C, lane 5) and the C-terminally tagged construct CH2705 (Fig. 1C, lane 6). Although CH2705 is not visualized by any antibody tested, this strain shows both *in vitro* and *in vivo* activity, which demonstrates that it is expressed (see below).

All of the Ste14p constructs are biochemically active *in vitro*, to varying degrees, as determined by a quantitative *in vitro* vapor diffusion methyltransferase assay (Fig. 1D) (14, 22). The assay mixture contains [¹⁴C]SAM as the methyl donor, the synthetic isoprenylated substrate AFC as the methyl acceptor, and the crude membrane fraction from strains expressing Ste14p as the source of methyltransferase activity. Both sub-

TABLE II
Kinetic constants for crude and purified His-Ste14p with AFC and AGGC as substrates

	$K_{m(\text{app})}^a$	V_{max}	Relative catalytic efficiency $V_{\text{max}}/K_{m(\text{app})}$	Specificity constant $k_{\text{cat}}/K_{m(\text{app})}$
	μM	$\text{pmol}/\text{min}/\text{mg}$	$\text{pmol}/\text{min}/\text{mg}/\mu\text{M}$	$10^4 \text{ M}^{-1} \text{ s}^{-1}$
His-Ste14p in crude membranes				
AFC	13.4 ± 0.8^c	770.2 ± 12.6	57.5	N/A ^b
AGGC	17.2 ± 1.0	1113 ± 21	64.7	N/A
Pure, reconstituted His-Ste14p				
AFC	3.0 ± 0.2	50782 ± 973	N/A	0.99
AGGC	3.2 ± 0.2	56667 ± 878	N/A	1.0

^a K_m values are reported as apparent values, since we cannot exactly determine the concentration of substrate accessible to the enzyme.

^b N/A, not applicable.

^c Error represents ± 1 S.E.

strates are present in saturating concentrations. Base labile counts transferred onto AFC are measured by scintillation counting and the specific IcmT activity is expressed as picomoles of methyl groups transferred per min per milligram of crude membrane protein. It is important to note that the constructs containing the tags at the N terminus (CH2703, CH2704, CH2707) are more active than their C-terminal counterparts (CH2706, CH2702, CH2705) (Fig. 1D), suggesting an important role of the C terminus in the activity of this enzyme that is somewhat compromised when tags are introduced. The untagged protein (CH2758) demonstrates a lower specific activity due to its reduced expression level (Fig. 1C, lane 11). We have also determined that membrane-associated Ste14p is resistant to proteolytic degradation and its enzymatic activity is highly stable even upon repeated freeze-thaw cycles (data not shown).

Epitope-tagged Ste14p Proteins Are Biologically Active in Vivo—In addition to the evidence from the *in vitro* methyltransferase activity assays above, all of Ste14p proteins are biologically active *in vivo*, as determined by the **a**-factor halo assay in *S. cerevisiae* (Fig. 1D, lower panel). Saturated cultures from the different strains were spotted onto a lawn of α -cells that are supersensitive to the pheromone **a**-factor (SM2375). Production of mature bioactive **a**-factor, which requires methylation by Ste14p, results in a clear zone, called a halo, that is indicative of growth inhibition of the lawn. The negative control mutant CH2714 (Δ Ste14 deletion containing the empty vector) clearly shows no halo formation. In contrast, all of our constructs (CH2702 to CH2707 and CH2758) transformed into SM1188 show halo formation comparable with the positive control strains, SM1058 and SM3495, which express wild-type levels of Ste14p or Ste14p on a multicopy expression plasmid under control of the endogenous STE14 promoter, respectively. This assay is extremely sensitive for detecting very small amounts of mature **a**-factor.

Purification Efforts Focus on the N-terminally Histidine- and Myc Epitope-tagged Ste14p (CH2704)—Although immunoblot analyses demonstrated that all of the Ste14p proteins were overexpressed at high levels, and all showed methyltransferase activity to varying degrees, the experiments described below use only strain CH2704. CH2704 expresses Ste14p that is N-terminally tagged with 10 histidine residues and the triple myc epitope (Fig. 1B). We refer to this protein simply as His-Ste14p. This construct was chosen for further experimentation for the following reasons: 1) Ste14p expressed in this strain consistently had the highest specific enzyme activity (Fig. 1D); 2) the protein is expressed at ~ 10 – 20 times the level of Ste14p in strain SM3495, which uses the endogenous STE14 promoter on a multicopy expression plasmid (data not shown); 3) in the linear range of the methyltransferase assay, membranes from strain CH2704 expressing this construct show a dramatic 15–20-fold increase in activity, compared with those derived from SM3495 (Fig. 1D), which nicely mirrors the ~ 20 -fold overex-

pression of Ste14p observed by immunoblot analysis; and 4) having both the myc and polyhistidine tags offers multiple options for detection and purification.

Substrate Preference of His-Ste14p in Crude Membranes—The activity of the His-Ste14p-containing membranes was assayed by the *in vitro* vapor diffusion methyltransferase assay with the minimal substrates AFC and AGGC (Table II). Values for the apparent K_m ($K_{m(\text{app})}$) and V_{max} for His-Ste14p with these compounds were obtained by fitting the data to the Michaelis-Menten equation using GraphPad Prism 4 (Table II). The $K_{m(\text{app})}$ values were $13.4 \pm 0.8 \mu\text{M}$ for AFC and $17.2 \pm 1.0 \mu\text{M}$ for AGGC. The V_{max} values were 770.2 ± 12.6 pmol of methyl groups transferred per min/mg for AFC and 1113 ± 21 pmol of methyl groups transferred per min/mg for AGGC. The preference of His-Ste14 for each substrate was determined by calculating the relative catalytic efficiency ($V_{\text{max}}/K_{m(\text{app})}$). It is not possible to calculate the actual specificity, $k_{\text{cat}}/K_{m(\text{app})}$, for these substrates, since the concentration of His-Ste14p enzyme in our crude membrane preparations is unknown. The relative catalytic efficiency for AFC was $57.5 \text{ pmol}/\text{min}/\text{mg}/\mu\text{M}$, and the relative catalytic efficiency for AGGC was $64.7 \text{ pmol}/\text{min}/\text{mg}/\mu\text{M}$. These data show that His-Ste14p in crude membrane preparations does not have a significant preference for either farnesyl or geranylgeranyl moieties in these substrates.

Detergent-solubilized His-Ste14p Is Enzymatically Active—To purify His-Ste14p, it was necessary to solubilize the protein from CH2704 crude membranes. A panel of detergents was screened to optimize for both efficient extraction of His-Ste14p from the crude cell membranes and for retention of enzymatic activity. This panel included non-ionic compounds, as well as zwitterionic and ionic detergents. Keeping the membrane protein concentration constant at 5 mg/ml, various detergents were tested at a final concentration of 1% (w:v). A starting concentration of membranes greater than 1 mg/ml was chosen to eliminate losses due to surface adsorption during the solubilization procedure (23). After solubilization and centrifugation at $300,000 \times g$ to remove unsolubilized material, the resultant supernatant fraction (post-spin) was examined for presence of His-Ste14p by immunoblot analysis (Fig. 2A) as well as for methyltransferase activity *in vitro* (Fig. 2B). The results were classified into three categories based on the extent of solubilization and the retention of enzymatic activity: 1) detergents that extracted His-Ste14p efficiently and retained methyltransferase activity, 2) detergents that extracted His-Ste14p efficiently but inactivated the enzyme, and 3) detergents that did not efficiently extract the protein. Under the conditions used in this study, the only detergent tested that was efficient at extracting the enzyme from the membrane at 1% (w:v) and that retained activity of His-Ste14p comparable with crude membranes was the non-ionic detergent DDM (Fig. 2 and Table III). DDM has proven effective in the purification of a number of other membrane proteins (24–26). Although some retention of activity was observed with Triton X-100,

none of other detergents were able to maintain the enzyme in an active form to any significant extent, despite effectively extracting His-Ste14p from the membrane.

Purification of Active His-Ste14p—Detergent-solubilized His-Ste14p was purified to homogeneity using metal affinity column chromatography (Fig. 3A and Table III) and its identity confirmed by immunoblot analysis (Fig. 3B). In brief, the purification scheme begins with the solubilization of the crude membranes in a buffer containing 20 mM imidazole and 1% DDM (pre-spin). After incubation for 1 h on ice, the non-solubilized and aggregated material was removed by centrifugation at $300,000 \times g$ for 30 min. The supernatant (post-spin), which contains the solubilized His-Ste14p, was incubated with Talon

metal affinity beads and the beads subsequently washed four times: two washes with buffer containing 40 mM imidazole and 1% DDM, one wash in the same buffer plus 0.5 M KCl, and finally one wash with buffer containing 40 mM imidazole, 0.5 M KCl, and 0.1% DDM. The washed beads were eluted in three fractions containing 0.1% DDM and 100 mM, 500 mM, or 1 M imidazole. The flow-through from the first column containing unbound material was incubated with fresh resin and washed and eluted as described above. The purified fractions were pooled and concentrated using a Microcon 30 concentrator (Millipore Co.). The His-Ste14p was purified to homogeneity as determined by silver nitrate stained SDS-PAGE gels (Fig. 3A). We have also confirmed the purity of the preparation and the identity of His-Ste14p by Edman degradation, where we detected only one N-terminal sequence that represented His-Ste14p (data not shown). We estimate that His-Ste14p comprises ~1–2% of the total membrane protein in the cell. Under the conditions used here, ~100 μ g of pure His-Ste14p is generated per 25 mg crude membrane proteins (derived from 3 liters of culture), representing up to a 30% yield of the total His-Ste14p starting material.

Reconstitution of Functional Purified His-Ste14p—Given that Ste14p is a multispanning membrane protein, we hypothesized that reconstitution of the purified material into lipid vesicles could be important for its activity. As a starting point, *E. coli* bulk lipids were used and liposomes were prepared using an extruder with 100-nm filters. A 100–1000-fold weight: weight excess of the liposomes was added directly to the purified His-Ste14p fractions after elution from the metal affinity column followed by a 20-fold rapid dilution in detergent-free buffer. This rapid detergent dilution method causes spontaneous reconstitution of membrane proteins into proteoliposomes and can result in a 1200–1500:1 lipid:protein molar ratio (20). We performed the *in vitro* methyltransferase assay on this reconstituted His-Ste14p to assess activity, using AFC as the methyl-accepting substrate. Activity in the purified fraction eluted from the metal affinity column was demonstrated, as well as an approximate 3–13-fold stimulation of the activity in the presence of lipid (0.17% w:v), depending upon the set of assay conditions used (Tables III and IV). Also, upon reconstitution into liposomes, the activity of the purified protein is enriched ~119-fold over the cell lysate as estimated by *in vitro* methyltransferase activity (Table III). To investigate whether distinct lipids would influence the activity of Ste14p, purified His-Ste14p was reconstituted with a wide variety of lipid and liposomal formulations containing *E. coli* bulk lipids, total extracts from egg and liver, phosphatidylethanolamine (PE) phosphatidylcholine (PC), phosphatidylserine (PS), and cholesterol (Table IV). In addition, a mixture of *E. coli* bulk lipids, PC, PS, and sterols in a ratio of 60:17.5:10:12.5 were used, an experimental condition previously successful for other polytopic membrane proteins (20). These data demonstrate that any lipid or lipid mixture tested was capable of supporting His-

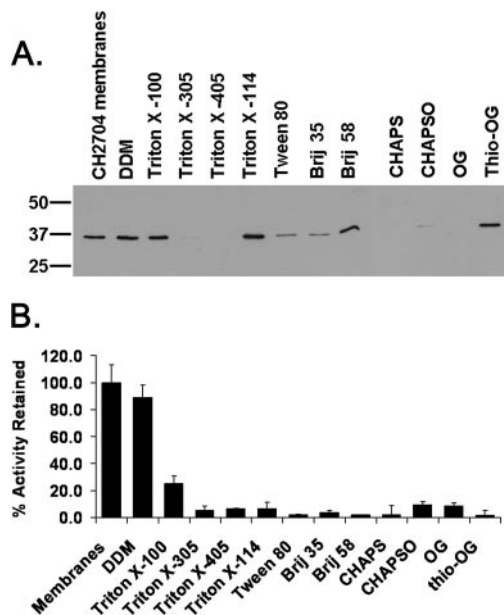


FIG. 2. Detergent screen for solubilizing His-Ste14p from crude membranes. Crude membranes containing His-Ste14p were solubilized in 1% of the indicated detergent followed by centrifugation at $300,000 \times g$ to pellet unsolubilized protein. The resultant supernatant (post-spin) was saved for analysis. **A**, one μ g of total protein from the crude His-Ste14p membranes and each post-spin were subjected to SDS-PAGE analysis, and His-Ste14p was visualized by immunodetection with an α -myc (1:10,000) antibody. Protein bands were visualized by enhanced chemiluminescence following incubation with HRP-conjugated α -mouse secondary antibody (1:4000). Data are representative of three experiments. **B**, total protein (5 μ g) from the crude His-Ste14p membranes and each post-spin were incubated with 20 μ M 14 C-SAM and 200 μ M AFC for 30 min at 30 $^{\circ}$ C and activity quantified by the *in vitro* vapor diffusion methyltransferase assay as described under “Experimental Procedures.” Activity is expressed as the percent activity retained after solubilization as compared with the crude membranes. Data are the average of three experiments done in duplicate. Error bars represent \pm 1 S.E. OG, *n*-octyl- β -D-glucopyranoside; thio-OG, *n*-octyl- β -D-thioglucopyranoside; CHAPSO, 3-[(3-cholamidopropyl)dimethylammonio]-2-hydroxy-1-propanesulfonate.

TABLE III
Purification of His-Ste14p

Fraction	Specific activity pmol/mg/min	Fold enrichment
Crude His-Ste14p cell lysate ^a	374 \pm 9	1
Crude His-Ste14p membranes ^a	909 \pm 16	2.4
Post-solubilization 300,000 \times g spin supernatant ^a	1408 \pm 33	3.8
Purified His-Ste14p reconstituted in <i>E. coli</i> liposomes ^b	45502 \pm 1661	119

^a The activity of His-Ste14p in 5 μ g of total protein from each fraction with 200 μ M AFC was quantified by the *in vitro* vapor diffusion methyltransferase assay as described under “Experimental Procedures.”

^b The initial concentration of AFC in the reaction mixture was 225 μ M. To more accurately assess activity, after the liposomes were incubated with AFC, excess substrate was removed by spin column gel filtration chromatography. The resultant concentration of AFC was 12.1 μ M, and activity was quantified using 0.089 μ g of purified His-Ste14p by the *in vitro* vapor diffusion methyltransferase assay as described under “Experimental Procedures.” Data are the average of three experiments done in duplicate. Error represents 1 S.E.

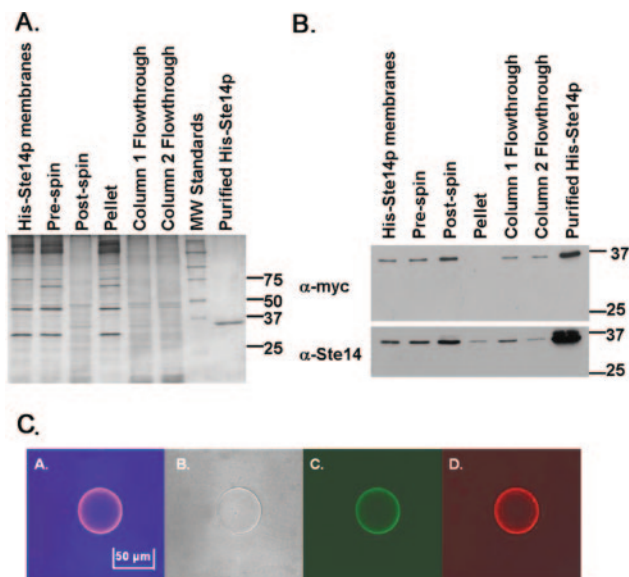


FIG. 3. Purification of detergent-solubilized His-Ste14p by metal affinity chromatography. Crude membranes containing His-Ste14p were solubilized in 1% DDM (*Pre-spin*) and spun at $300,000 \times g$ for 30 min to pellet unsolubilized protein (*Pellet*). The resultant supernatant (*Post-spin*) was incubated with Talon metal affinity resin (Clontech). After incubation, the flow-through (*column 1*, unbound) was incubated with fresh Talon metal affinity resin. The second flow-through (*column 2*, unbound) was discarded and the resin eluted with 100 mM, 500 mM, and 1 M imidazole-containing buffer. The elution fractions were combined and concentrated. **A**, total protein (5 μ g) from each fraction and 1 μ g of total purified His-Ste14p were subjected to 12% SDS-PAGE analysis and silver staining. **B**, total protein (1 μ g) from each fraction and 100 ng of purified His-Ste14p were subjected to 12% SDS-PAGE analysis, and Ste14p was visualized by immunodetection with either α -myc monoclonal antibody (1:10,000) or α -Ste14 polyclonal antibody (1:1000). Bands were visualized by enhanced chemiluminescence following incubation with HRP-conjugated secondary antibodies (α -mouse, 1:4000 for α -myc and α -rabbit, 1:10000 for α -Ste14). Data are representative of several experiments. **C**, confocal microscope images of purified and reconstituted His-Ste14p. Purified His-Ste14p (~ 1 – 2μ g in 3 μ l of 500 mM imidazole elution buffer) was diluted to a final volume of 60 μ l in buffer containing 100 mM Tris-HCl, pH 7.5, and 100 μ g of non-extruded *E. coli* polar lipid extract (Avanti Polar Lipids, Inc.). The sample was stained with an anti-myc monoclonal antibody and visualized with a fluorescein isothiocyanate-conjugated goat-anti-mouse secondary antibody (**C**) and with Nile Blue, a lipid stain with red fluorescence (**D**). The images were visualized at $60\times$ magnification. **B** represents the non-fluorescent confocal transmission image of the vesicle, and **A** is the merged image of **B**–**D**.

Ste14p activity (Table IV). Upon treatment of the 100-nm vesicles with alamethicin, a compound that permeabilizes membranes, we observed a $\sim 20\%$ increase in activity (data not shown). These data suggest that $\sim 80\%$ of the vesicles have the active site oriented outward.

To confirm the presence of vesicles containing reconstituted His-Ste14p after rapid dilution in the presence of exogenous non-extruded bulk *E. coli* lipids, we performed confocal immunofluorescence microscopy using an anti-myc antibody (Fig. 3C). These data corroborate our findings that His-Ste14p is reconstituted into lipid vesicles. These vesicles range in size from 20–60 μ m in diameter, and under these conditions, His-Ste14p appears to be uniformly distributed in the lipid membrane.

Purified and Reconstituted Ste14p Does Not Prefer AFC over AGGC—The saturation curves for AFC and AGGC as substrates were performed using purified His-Ste14p reconstituted in *E. coli* bulk polar lipid liposomes (100-nm diameter). Since we hypothesized that any excess substrate would further skew the kinetic results, we used an approach that removes unincorporated substrate from the liposomes (see also “Exper-

imental Procedures”) (Table II). Extruded liposomes doped with 0.05% Texas Red-labeled 1,2-dihexadecanoyl-*sn*-glycero-3-phosphoethanolamine were incubated with increasing amounts of either AFC or AGGC and subjected to gel filtration spin column chromatography. Extruded liposomes were first made and then incubated with isoprenylated substrate to minimize encapsulation of substrate. Spin gel filtration columns were used to minimize the separation time and thus minimize substrate dissociation from the liposomes (27). The recovery of the liposomes was monitored spectrophotometrically and was determined to be virtually complete ($100 \pm 5\%$). We then determined an accurate concentration of substrate in each liposomal fraction spectrophotometrically and found that only ~ 3 – 7% of the initial concentration of substrate added remained associated with the liposomes. Aliquots of the same liposome-substrate fractions were subjected to the *in vitro* methyltransferase assay, and the data were fitted to the Michaelis-Menten equation using GraphPad Prism 4 (Table II). The $K_{m(\text{app})}$ values were $3.0 \pm 0.2 \mu\text{M}$ for AFC and $3.2 \pm 0.2 \mu\text{M}$ for AGGC. The V_{max} values were 50782 ± 973 pmol of methyl groups transferred per min/mg for AFC and $56,667 \pm 878$ pmol of methyl groups transferred per min/mg for AGGC. We also calculated the specificity constant ($k_{\text{cat}}/K_{m(\text{app})}$) and determined that there is no statistically significant difference between the specificity constants obtained for AFC ($0.99 \times 10^4 \text{ M}^{-1} \text{ s}^{-1}$) or AGGC ($1.0 \times 10^4 \text{ M}^{-1} \text{ s}^{-1}$). These data indicate that His-Ste14p has no preference for AGGC over AFC under our assay conditions.

Optimal pH for Reconstituted His-Ste14p—The specific activity of reconstituted His-Ste14p was determined over a range of pH values by the *in vitro* vapor diffusion methyltransferase assay (Fig. 4). The optimal pH for maximal specific activity was 7.0 in MES. The specific activity dropped off rapidly below pH 6.5 and more slowly above pH 8.0. These results are similar to those obtained using crude His-Ste14p-containing membranes, where the optimal pH for maximal specific activity was 7.5 (data not shown), and are consistent with the cytosolic localization of much of the non-membrane-associated domains of the enzyme. These data are comparable with those obtained for the enzyme from rat liver crude membranes, which demonstrated a pH optimum near 7.0 (28).

Inhibition of Reconstituted His-Ste14p by Metal Chelators—We and others (29) have preliminary evidence that Ste14p and mammalian Icmt are dependent upon metals for activity. Treatment of crude membranes with *o*-phenanthroline (OP) eliminates catalytic activity of His-Ste14p, presumably by chelation of the metal ligand from the enzyme (29).² We have further characterized the metal dependence of His-Ste14p by treating the purified and reconstituted protein with a panel of chelating agents at 10 mM and examining methyltransferase activity *in vitro* (Fig. 5A). An inhibition curve of purified reconstituted His-Ste14p by 2-carboxy-2'-hydroxy-5'-sulfoformazylbenzene (Zincon) demonstrates an IC_{50} of 1.1 mM with a 95% confidence interval of 1.0–1.3 mM as determined by fitting of the inhibition curve to a sigmoidal dose-response curve using GraphPad Prism 4 (Fig. 5B). A non-linear Dixon plot of 1/specific activity versus concentration demonstrates a hyperbolic line, which is indicative of irreversible inhibition (Fig. 5B, inset) (30). Notably, Zincon, the most hydrophobic of the chelators examined, was the most potent inhibitor of His-Ste14p, suggesting the metal ion is buried in a water-insoluble environment. Similar inhibition was observed by these metal chelators in crude membrane preparations of untagged Ste14p, suggesting that the presence of the polyhistidine tag is not responsible for the effects (data not shown).

² W. Schmidt and S. Michaelis, data not shown.

TABLE IV
His-Ste14p reconstitution in liposomes of various composition

Pure His-Ste14p was reconstituted into liposomes. Specific activities were determined by *in vitro* vapor diffusion methylation assays as described under "Experimental Procedures." All data are the average of at least three experiments. Error represents 1 S.E.

Composition	Specific activity	% ^a
	<i>pmol/mg/min</i>	
Pure His-Ste14p	3602 ± 225	33.8
<i>E. coli</i> liposomes	10,645 ± 232	100.0
Egg extract	8492 ± 366	79.8
Liver extract	6690 ± 550	62.8
Egg extract/cholesterol (85:15)	7913 ± 463	74.3
Egg PC	8263 ± 583	77.6
Egg PC/egg PE (50:50)	7955 ± 368	74.7
<i>E. coli</i> /egg PC/brain PS/cholesterol (60:17.5:10:12.5)	10,690 ± 304	100.4
Egg PC/cholesterol (85:15)	8977 ± 308	84.3
Egg PC/brain PS (50:50)	8884 ± 681	83.5
Brain extract	8351 ± 853	78.4
Heart extract	10,665 ± 810	100.2
Egg PC/egg PA (50:50)	8623 ± 466	81.0
Egg PC/egg PE/bovine liver PI/brain PS (51:19:23:7)	8943 ± 951	84.0
PC/PE/PI/PS/cholesterol (43:16:20:6:15)	7963 ± 677	74.5

^a Percent as normalized to the value for liposomes prepared from *E. coli* bulk polar lipid.

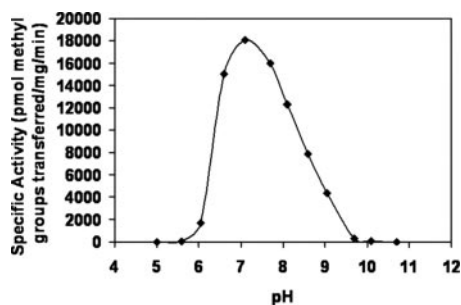


FIG. 4. pH dependence of His-Ste14p. Purified His-Ste14p (0.39 μ g) was reconstituted in 100 μ g of *E. coli* 100-nm liposomes in the presence of 200 μ M AFC as described under "Experimental Procedures" using the following buffers at a final concentration of 100 mM: MES (pH 5–7), Tris-HCl (pH 7.5–9), and NaHCO₃ (pH 9.5–11). Reactions were carried out for 30 min at 30 °C following addition of 20 μ M ¹⁴C-SAM. Activity was quantified by the *in vitro* vapor diffusion methyltransferase assay as described under "Experimental Procedures." Data are the average of three experiments performed in duplicate. Error bars represent \pm 1 S.E.

Farnesylated and AAX-proteolyzed His-Ras2p Is an in Vitro Substrate for Purified and Reconstituted His-Ste14p—We have expressed and purified yeast Ras2p tagged with a 10-histidine repeat followed by a triply iterated *myc* epitope at the N terminus (His-Ras2p) in a Δ *ste14* deletion strain of *S. cerevisiae*. Expression in the *ste14* deletion strain provides us with isoprenylated and C-terminally proteolyzed but not methylated His-Ras2p that should serve as a protein substrate for Ste14p-mediated carboxyl methylation. His-Ras2p was purified using metal affinity chromatography, and the identity of His-Ras2p was confirmed by immunoblotting with an anti-*myc* antibody (data not shown). This enriched preparation of His-Ras2p was assayed as a substrate for purified His-Ste14p, and the specific activity of His-Ras2p was \sim 170 times greater than the negative control, demonstrating that His-Ras2p is a substrate for His-Ste14p *in vitro* (Fig. 6).

DISCUSSION

Integral membrane proteins are notoriously refractory to purification in an active form. In the course of this study, we have developed a system for the overexpression, purification, and characterization of a multispansing integral membrane protein in yeast, which could be used for other such membrane proteins. We demonstrate here the successful optimization, solubilization, and purification of His-Ste14p from CH2704 cells using 1% *n*-dodecyl- β -D-maltopyranoside and metal affin-

ity chromatography. We have made the key finding that Ste14p, after detergent-solubilization with 1% DDM, retains its biochemical methyltransferase activity *in vitro* (Table III and Fig. 2) and exhibits normal saturation curve kinetics (data not shown). This is a significant accomplishment because previous attempts to maintain Icmt activity upon solubilization with numerous other detergents met with limited to no success (9, 31). Some success with CHAPS, however, has been reported for the partial purification of the Icmt from bovine brain (32). Our previous studies with yeast Ste14p expressed in *E. coli* suggested that it acts alone (15). The results presented here with the purified enzyme prove that Ste14p is the sole component of the methyltransferase activity.

Our expression and purification conditions allow us to generate a substantial amount of pure protein (\sim 100 μ g of pure His-Ste14p per 25 mg of crude membrane proteins, which can represent up to a 30% yield of the total His-Ste14p starting material). Given the ease of growing large quantities of yeast cells, we have also successfully scaled up this purification procedure. We can now easily obtain between 0.5–1 mg of pure active His-Ste14p per purification. Furthermore, the purified protein is not affected substantially by repeated freeze-thaw cycles. This impressive stability, coupled with the small size of Ste14p (239 aa) and the finding that it is active when solubilized in detergent, argues well for Ste14p as an excellent candidate for further biochemical and biophysical analyses and crystallization trials. Experiments are currently underway to increase yield of the His-Ste14p to obtain the much larger quantities needed for crystallization trials. Importantly, we have also shown that an enriched preparation of His-Ras2p is a substrate for purified and reconstituted His-Ste14p *in vitro*. Further purification of His-Ras2p protein to homogeneity will be an invaluable tool for further characterization of Icmt, as it will allow us to more accurately determine a $K_{m(\text{app})}$ as well as to probe whether there are specificity determinants within the protein substrate itself. In addition, although not yet purified, we have overexpressed enzymatically active human Icmt in yeast to high levels using the vectors and strains described here.

Reconstitution of His-Ste14p into lipid or liposomes enhanced the enzymatic activity. Given that alterations in lipid composition have little effect on activity for AFC, we propose that the interaction of the lipophilic substrate and the active site of the enzyme are not influenced profoundly by the nature of the surrounding lipid environment and hypothesize that the

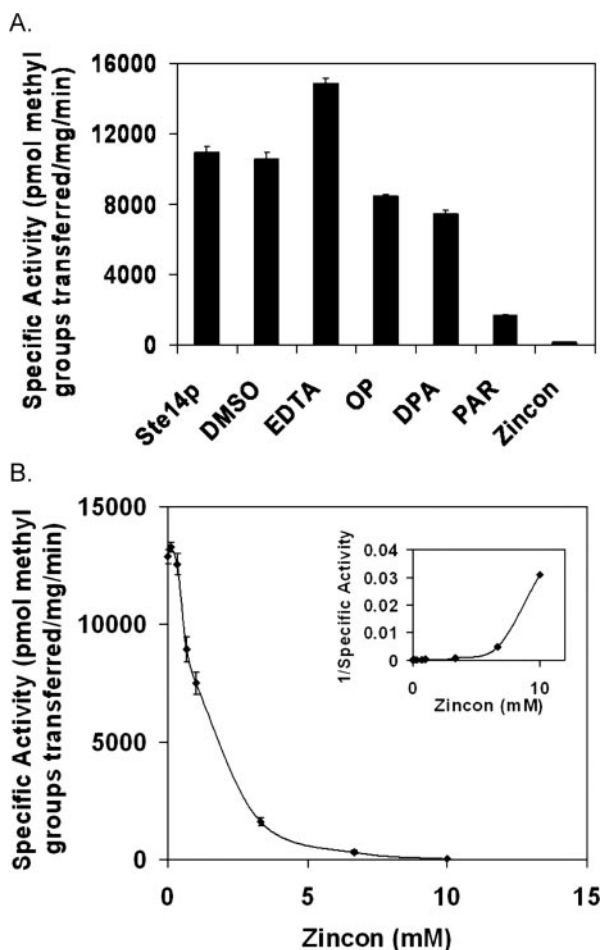


FIG. 5. Inhibition of reconstituted His-Ste14p activity by metal chelating compounds. A, purified His-Ste14p (0.39 μg) was reconstituted in 100 μg of *E. coli* 100-nm liposomes in the presence of 133 μM AFC as described under "Experimental Procedures." The His-Ste14p-containing liposomes were preincubated with a 10 mM concentration of the indicated inhibitor (100 mM stock in Me_2SO (DMSO) except EDTA, pH 8.0, in water) for 10 min at 30 $^\circ\text{C}$, prior to addition of 20 μM ^{14}C -SAM. The Me_2SO sample contains 6 μl of Me_2SO as a solvent control. Reactions were carried out for 30 min at 30 $^\circ\text{C}$ and activity quantified by the *in vitro* vapor diffusion methyltransferase assay as described under "Experimental Procedures." *E. coli* liposomes containing no protein were subjected to the same conditions without inhibitor and the activity subtracted from those with protein. Data are the average of two experiments done in duplicate. Error bars represent ± 1 S.E. B, inhibition of reconstituted His-Ste14p activity by Zincon. Purified His-Ste14p (0.39 μg) was assayed as described for A with the indicated concentration of Zincon (stock in Me_2SO) for 10 min at 30 $^\circ\text{C}$, prior to addition of 20 μM ^{14}C -SAM. The 0 mM sample contains 6 μl of Me_2SO as a solvent control. Reactions were carried out for 30 min at 30 $^\circ\text{C}$ and activity quantified by the *in vitro* vapor diffusion methyltransferase assay as described under "Experimental Procedures." *E. coli* liposomes containing no protein were subjected to the same conditions without Zincon and the activity subtracted from those with protein. Inset, Dixon plot of 1/specific activity. Data are the average of two experiments done in duplicate. Error bars represent ± 1 S.E. DPA, 2,6-pyridinedicarboxylic acid; PAR, 4-(2-pyridylazo)resorcinol.

binding site for the lipophilic substrate lies within the trans-membrane helices of the enzyme.

His-Ste14p in crude membrane preparations does not appear to show a preference for either farnesylated or geranylgeranyl-ated minimal substrates (Table II), in accordance with a previous study using bovine retinal rod membranes (33). In contrast, however, Icmt from human neutrophil membranes appeared to prefer AGGC to AFC by a factor of ~ 10 -fold (31). Furthermore, a previously published report suggests that the Icmt from *Trypanosoma brucei* has a preference for AFC over

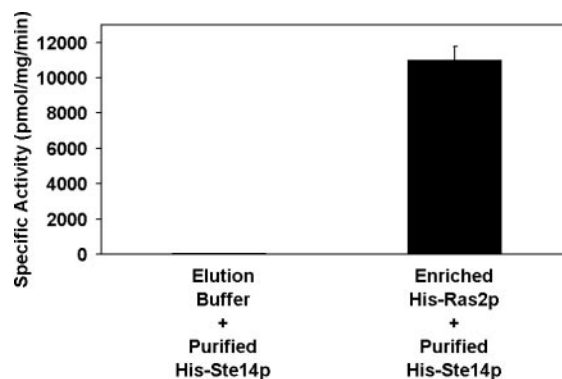


FIG. 6. Partially purified His-Ras2p as a purified and reconstituted His-Ste14p substrate. Total protein (94 μg) from the partial purification of His-Ras2p and 0.11 μg of purified His-Ste14p were incubated with 20 μM ^{14}C -SAM for 30 min at 30 $^\circ\text{C}$. The activity was quantified by the *in vitro* vapor diffusion methyltransferase assay as described under "Experimental Procedures." Data are the average of two experiments done in duplicate. Error bars represent ± 1 S.E.

AGGC, although the degree of preference depended on the amount of membranes used in the enzymatic assays (34). These data led to the speculation that with a larger quantity of membranes present in the assay, more AFC would be partitioned to the lipid and become available for use by the enzyme (34). By this rationale, it was difficult to ascertain whether the catalytic efficiencies determined in crude membranes truly demonstrate the preference of the enzyme or if they reflect the ability of the substrates to partition into the membranes. In this study, we have overcome this problem by performing detailed kinetic analyses with the purified enzyme using AFC and AGGC as substrates. Our initial kinetic experiments in which we did not separate free substrate from that incorporated into liposomes yielded $K_{m(\text{app})}$ values that were higher than expected. These data suggested that there is a 3-fold preference for AGGC over AFC (data not shown). However, these data could have resulted simply from the fact that the liposomes did not contain equal amounts of prenylated substrate in the liposomes.

Therefore, we devised an assay to ensure that we could both quantitate the amount of substrate in the liposomes and avoid the complicating effects of excess substrate. We incubated the liposomes with substrate after extrusion to limit the amount of isoprenylated substrate trapped within the liposomes themselves (27) and then removed substrate not associated with the liposomes by rapid gel filtration spin column chromatography. This procedure yielded nearly 100% recovery of the liposomes. We were also careful to accurately determine the final concentration of either AFC or AGGC in the recovered liposomes spectrophotometrically. From these data, we determined that the V_{max} and $K_{m(\text{app})}$ values for the two substrates are similar ($\sim 50,000$ – $56,000$ pmol of methyl groups transferred per min/mg and 3.0–3.2 μM , AFC and AGGC, respectively) and that the specificity constants were equivalent, within experimental error, supporting the hypothesis that Ste14p does not prefer farnesyl moieties over geranylgeranyl moieties, at least in these small model substrates (Table II).

Icmt from rat kidney has been reported to be a metalloenzyme (29). We have now determined that purified and reconstituted His-Ste14p is also sensitive to the chelators 4-(2-pyridylazo)resorcinol and Zincon, and to *o*-phenanthroline to a lesser degree, thus suggesting that it is a metal dependent enzyme (Fig. 5). Interestingly, the degree of inhibition mirrored the hydrophobicity of the chelator. For example, the water-soluble chelator EDTA was incapable of inhibiting His-Ste14p up to a concentration of 300 mM (data not shown). However, the more hydrophobic compounds OP and Zincon were more effective at

lower concentrations. Whereas OP had minimal inhibitory effects at 10 mM, by 50 mM the inhibition was complete (Fig. 5 and data not shown). These data suggest that the local environment surrounding the metal ion is hydrophobic. Furthermore, the inhibition by Zincon suggests the presence of either copper or zinc in the enzyme but does not conclusively rule out other metals (30, 35). We are currently attempting to identify the metal from the purified enzyme using inductively coupled plasma mass spectrometry (ICPMS) and determining the identity of the chelating amino acid ligands.

Proteolytic protection studies further suggested that the metal plays a structural and stabilizing role rather than a catalytic role in the enzyme (29). This hypothesis is supported by the data presented here showing the apparent irreversibility of His-Ste14p inhibition by Zincon (Fig. 5B). In addition, attempts at adding back metal ions, such as zinc, after chelation did not reactivate the enzyme (data not shown). In fact, the addition of exogenous zinc to the untreated enzyme caused a profound inhibition of enzyme activity (data not shown). Presumably, loss of the structural metal ion causes reduction of His-Ste14p activity due to an irreversible conformational change in the enzyme.

It is interesting to note that all of the enzymes involved in the post-translational C-terminal processing of CAAX proteins have been shown or are predicted to be metalloenzymes (25, 36–39). These components include the soluble farnesyl- and geranylgeranyltransferase, the ER-integral membrane “AAXing” endoproteases Ste24p or Rce1p that cleave the three C-terminal residues, and the ER-integral membrane Icm1. An attractive hypothesis is that all of these components interact (stably or transiently) to form a CAAX modification complex at the ER-cytoplasmic interface. CAAX substrates could be passed efficiently from enzyme to enzyme before they are targeted to their ultimate cellular locations. It is also interesting to speculate that this complex of enzymes might share a common metal delivery system that facilitates their regulation in concert.

Recently, potent farnesyltransferase (FTase) inhibitors have been developed as potential cancer chemotherapeutic agents. A subset of these agents has exhibited promise as anti-cancer agents in human clinical trials. These inhibitors are thought to have multiple cellular targets, including some Ras proteins. Importantly, K-Ras can be alternatively geranylgeranylated in the presence of FTase inhibitors, whereas H-Ras is not (40, 41). Due to this alternate prenylation, K-Ras-driven tumors are, in general, much more resistant to FTase inhibitors than H-Ras driven tumors (42, 43). K-Ras is the most commonly mutated form of Ras found in human malignancies, particularly in solid malignancies (44). K-Ras is mutated in over 90% of all pancreatic cancers, 40–50% of colon cancers, and 25% of ovarian cancers (44). Recent studies with Icm1^{-/-} fibroblast have indicated that the methylation of oncogenic K-Ras and B-Raf proteins by Icm1 plays a central role in the cellular localization and transformation ability of these key oncoproteins (10, 13). Combined, these data provide compelling reasons that inhibitors of Icm1 have great potential as novel anti-cancer agents. Because Icm1 recognizes both farnesylated and geranylgeranylated proteins, we believe that Icm1 inhibitors will afford us a way to target resistant K-Ras tumors alone or in conjunction with existing FTase inhibitors.

Acknowledgments—We thank Dr. Jennifer S. Laurence and Heather B. Hodges for assistance with plasmid construction and initial protein expression and Gregory Huyer, David Thompson, and Jennifer Hovis for advice.

REFERENCES

- Zhang, F. L., and Casey, P. J. (1996) *Annu. Rev. Biochem.* **65**, 241–269
- Young, S. G., Ambroziak, P., Kim, E., and Clarke, S. (eds) (2000) *The Enzymes*, 3rd Ed., Vol. 21, pp. 155–213, Academic Press, San Diego, CA
- Hrycyna, C. A., and Clarke, S. (1993) *Pharmacol. Ther.* **59**, 281–300
- Volker, C., Lane, P., Kwee, C., Johnson, M., and Stock, J. (1991) *FEBS Lett.* **295**, 189–194
- Schmidt, W. K., Tam, A., Fujimura-Kamada, K., and Michaelis, S. (1998) *Proc. Natl. Acad. Sci. U. S. A.* **95**, 11175–11180
- Dai, Q., Choy, E., Chiu, V., Romano, J., Slivka, S. R., Steitz, S. A., Michaelis, S., and Philips, M. R. (1998) *J. Biol. Chem.* **273**, 15030–15034
- Hrycyna, C. A., Sapperstein, S. K., Clarke, S., and Michaelis, S. (1991) *EMBO J.* **10**, 1699–1709
- Romano, J. D., Schmidt, W. K., and Michaelis, S. (1998) *Mol. Biol. Cell* **9**, 2231–2247
- Stephenson, R. C., and Clarke, S. (1992) *J. Biol. Chem.* **267**, 13314–13319
- Bergo, M. O., Leung, G. K., Ambroziak, P., Otto, J. C., Casey, P. J., and Young, S. G. (2000) *J. Biol. Chem.* **275**, 17605–17610
- Winter-Vann, A. M., Kamen, B. A., Bergo, M. O., Young, S. G., Melnyk, S., James, S. J., and Casey, P. J. (2003) *Proc. Natl. Acad. Sci. U. S. A.* **100**, 6529–6534
- Sapperstein, S., Berkower, C., and Michaelis, S. (1994) *Mol. Cell. Biol.* **14**, 1438–1449
- Bergo, M. O., Gavino, B. J., Hong, C., Beigneux, A. P., McMahon, M., Casey, P. J., and Young, S. G. (2004) *J. Clin. Invest.* **113**, 539–550
- Hrycyna, C. A., and Clarke, S. (1990) *Mol. Cell. Biol.* **10**, 5071–5076
- Hrycyna, C. A., Wait, S. J., Backlund, P. S., Jr., and Michaelis, S. (1995) *Methods Enzymol.* **250**, 251–266
- Romano, J. D., and Michaelis, S. (2001) *Mol. Biol. Cell* **12**, 1957–1971
- Kagan, R. M., and Clarke, S. (1994) *Arch. Biochem. Biophys.* **310**, 417–427
- Elble, R. (1992) *BioTechniques* **13**, 18–20
- Schaffner, W., and Weissmann, C. (1973) *Anal. Biochem.* **56**, 502–514
- Ambudkar, S. V., Lelong, I. H., Zhang, J., and Cardarelli, C. (1998) *Methods Enzymol.* **292**, 492–504
- Trueblood, C. E., Boyartchuk, V. L., Picologlou, E. A., Rozema, D., Poulter, C. D., and Rine, J. (2000) *Mol. Cell. Biol.* **20**, 4381–4392
- Ota, I. M., and Clarke, S. (1989) *J. Biol. Chem.* **264**, 12879–12884
- Hjelmeland, L. M. (1990) *Methods Enzymol.* **182**, 253–264
- Lerner-Marmarosh, N., Gimi, K., Urbatsch, I. L., Gros, P., and Senior, A. E. (1999) *J. Biol. Chem.* **274**, 34711–34718
- Tam, A., Schmidt, W. K., and Michaelis, S. (2001) *J. Biol. Chem.* **276**, 46798–46806
- Ketchum, C. J., Schmidt, W. K., Rajendrakumar, G. V., Michaelis, S., and Maloney, P. C. (2001) *J. Biol. Chem.* **276**, 29007–29011
- Silvius, J. R., and l'Heureux, F. (1994) *Biochemistry* **33**, 3014–3022
- Stephenson, R. C., and Clarke, S. (1990) *J. Biol. Chem.* **265**, 16248–16254
- Desrosiers, R. R., Nguyen, Q. T., and Beliveau, R. (1999) *Biochem. Biophys. Res. Commun.* **261**, 790–797
- Siemann, S., Brewer, D., Clarke, A. J., Dmitrienko, G. I., Lajoie, G., and Viswanatha, T. (2002) *Biochim. Biophys. Acta* **1571**, 190–200
- Pillinger, M. H., Volker, C., Stock, J. B., Weissmann, G., and Philips, M. R. (1994) *J. Biol. Chem.* **269**, 1486–1492
- Yoo, B. C., Kang, M. S., Kim, S., Lee, Y. S., Choi, S. Y., Ryu, C. K., Park, G. H., and Han, J. S. (1998) *Exp. Mol. Med.* **30**, 227–234
- Perez-Sala, D., Gilbert, B. A., Tan, E. W., and Rando, R. R. (1992) *Biochem. J.* **284**, 835–840
- Buckner, F. S., Kateete, D. P., Lubega, G. W., Van Voorhis, W. C., and Yokoyama, K. (2002) *Biochem. J.* **367**, 809–816
- Richter, P., Toral, M. I., Tapia, A. E., and Fuenzalida, E. (1997) *Analyst* **122**, 1045–1048
- Park, H. W., Boduluri, S. R., Moomaw, J. F., Casey, P. J., and Beese, L. S. (1997) *Science* **275**, 1800–1804
- Fu, H. W., Beese, L. S., and Casey, P. J. (1998) *Biochemistry* **37**, 4465–4472
- Hightower, K. E., and Fierke, C. A. (1999) *Curr. Opin. Chem. Biol.* **3**, 176–181
- Pei, J., and Grishin, N. V. (2001) *Trends Biochem. Sci.* **26**, 275–277
- Whyte, D. B., Kirschmeier, P., Hockenberry, T. N., Nunez-Oliva, I., James, L., Catino, J. J., Bishop, W. R., and Pai, J. K. (1997) *J. Biol. Chem.* **272**, 14459–14464
- Rowell, C. A., Kowalczyk, J. J., Lewis, M. D., and Garcia, A. M. (1997) *J. Biol. Chem.* **272**, 14093–14097
- Cox, A. D., and Der, C. J. (1997) *Biochim. Biophys. Acta* **1333**, F51–F71
- Cox, A. D. (2001) *Drugs* **61**, 723–732
- Adjei, A. A. (2001) *J. Natl. Cancer Inst.* **93**, 1062–1074
- Michaelis, S., and Herskowitz, I. (1988) *Mol. Cell. Biol.* **8**, 1309–1318
- Hitzeman, R. A., Chen, C. Y., Hagie, F. E., Patzer, E. J., Liu, C. C., Estell, D. A., Miller, J. V., Yaffe, A., Kleid, D. G., Levinson, A. D., and Oppermann, H. (1983) *Nucleic Acids Res.* **11**, 2745–2763
- Berkower, C., Taglicht, D., and Michaelis, S. (1996) *J. Biol. Chem.* **271**, 22983–22989